

Provided for non-commercial research and education use.
Not for reproduction, distribution or commercial use.



This article appeared in a journal published by Elsevier. The attached copy is furnished to the author for internal non-commercial research and education use, including for instruction at the authors institution and sharing with colleagues.

Other uses, including reproduction and distribution, or selling or licensing copies, or posting to personal, institutional or third party websites are prohibited.

In most cases authors are permitted to post their version of the article (e.g. in Word or Tex form) to their personal website or institutional repository. Authors requiring further information regarding Elsevier's archiving and manuscript policies are encouraged to visit:

<http://www.elsevier.com/copyright>



Contents lists available at ScienceDirect

Thin Solid Films

journal homepage: www.elsevier.com/locate/tsf

Formation of CoN_x ultra-thin films during direct-current nitrogen ion sputtering in ultrahigh vacuum

Chiung-Wu Su^{*}, Yen-Chu Chang, Tsung-Hsuan Tsai, Sheng-Chi Chang, Ming-Siang Huang

Department of Electrophysics, National Chiayi University, 300 Syuefu Rd., Chiayi 60004, Taiwan

ARTICLE INFO

Article history:

Received 23 March 2010

Received in revised form 23 January 2011

Accepted 25 January 2011

Available online 2 February 2011

Keywords:

Ultra-thin films

Sputtering

Ion implantation

Auger electron spectroscopy (AES)

Nitrides

ABSTRACT

This study reports the formation of ultra-thin cobalt nitride (CoN_x) films on a $\text{Co/ZnO}(002)$ crystal by low-energy ion sputtering of nitrogen in an ultrahigh vacuum system. The CoN_x film formed during ion bombardment in which the nitrogen plasma (N^+) results in both sputtering and implantation in the formation process of CoN_x , especially for the Co adsorbed layers. Auger electron spectroscopy analysis shows that the composition ratio x as a function of sputtering time was highly related to the N^+ ion energy that was varied from 0.5 to 2 keV. The composition ratio x of CoN_x films is inversely proportional to the ion energy. Low-energy ion sputtering is possible to fabricate ultra-thin CoN_x films and to adjust their chemical compositions.

© 2011 Elsevier B.V. All rights reserved.

1. Introduction

The ion collision caused by sputtering surface layers on a solid surface is an important issue in solid-state sciences [1]. From a microscopic point of view, charge-transfer and ion-molecule reactions should influence low-energy ion transport through ultra-thin films. As the projectile ions pass through a molecular overlayer, they may interact with the overlayer molecules via charge transfer. These chemical reactions may form new species [2,3]. Implantation techniques can help reveal the microscopic properties of materials, and tailor the surface properties of metal components for specialized applications [4]. Plasma source ion implantation is an effective surface modification method [5]. However, the ion energy required for ion implantation typically exceeds 10 keV [6–9]. Previous studies raise critical questions about doping and damaging effects in materials [10,11]. Reducing the thickness of films is a necessary step in eliminating the uncertainty effect caused by thick films, determining their physical properties and reducing complexity of segregation effect between layers. Instead, the production of ultra-thin films is the motivation of this study. Cobalt nitride (Co-N) is a multifunctional material widely used in the interconnects of integrated circuits [12], metal catalysts [13], and hydrazine decomposition [14]. Though this material can be fabricated from various chemical methods or deposited via pulsed laser deposition, it is typically only used for producing thick films. Relatively few studies report films with a thickness on the nanometer scale or use physical deposition methods

such as ion sputtering. Unlike the traditional sputtering method, which uses radio-frequency ion-generated power in a high-pressure vacuum [15]; this study uses low-energy ion sputtering involving an electron bombarded ion source under a vacuum around 10^{-4} Pa [16]. This makes it possible to form ultra-thin Co-N films by the nitrogen ion (N^+) in the sputtering technique. Previous results indicate that the stoichiometric compound Co_3N_2 might exist in the amorphous phase in very special conditions with a low ion current to target ($13.5 \mu\text{A}$) [17]. Nevertheless, the compositional ratio x of non-stoichiometric CoN_x films in the current study is strongly dependent on the incident ion energy with a higher ion current ($20 \mu\text{A}$). A sputtering effect (removal of Co adsorbate) accompanies the implantation effect (CoN_x phase formation) in the formation of Co-N ultra-thin films. The advantage of this study is to use the key method to tune the thickness of the nitride film in the ultra-thin film structure.

2. Experimental

The experiments in this study were performed in an ultrahigh vacuum (UHV) with a base background pressure of approximately 2×10^{-8} Pa. The substrate $\text{ZnO}(002)$ was an N-type commercial crystal with a cubic dimension of $10 \times 10 \times 0.5 \text{ mm}^3$. Cobalt films were epitaxially deposited by a home-made thermal evaporator while resistance heating of the 0.5 mm Co filament in UHV. The electric power of the evaporator was maintained at approximately 16 W to stabilize the deposition rate of Co atomic flux. The chemical composition of samples was determined by SPECTAVIEW LEED/Auger electron spectroscopy (AES) with a 4-grid retarding field analyzer manufactured from Omicron Co. Ltd. The nitrogen plasma source was an ISE-10 ion gun manufactured by Omicron Co. Ltd. The angle of the ion incidence was

^{*} Corresponding author. Tel.: +886 5 2717905; fax: +886 5 2717909.
E-mail address: cwsu@mail.ncyu.edu.tw (C.-W. Su).

normal to the surface. The bombarded energy can be adjusted from 0.5 to 4 keV with a 10 mA thermal electron beam and 20 μA ion current with respect to the target. The ion flux density estimated from the surface with a cleaned circular shape on the other side of the copper sample holder was approximately 1.3×10^{14} ions/cm² s.

2.1. Preparation of a clean ZnO(002) substrate and determination of surface type

The ZnO(002) substrate used in this study was a transparent crystal with a light yellow appearance. According to the instructions on the commercial packaging of the sample, the surface before use is Zn-terminated on one side and O-terminated on the other side. The experiments in this study initially chose the O-terminated face as the substrate because it may provide information for further magnetic research. Since the surface structure of the substrate is somewhat irrelevant, the goal of this study is to generate an ultra-thin amorphous layer on the surface. After bombardment, the disordered surface may be a suitable template for the study. Like most experiments in surface science, the substrate was first cleaned with Ar⁺ plasma to remove surface contaminants such as carbon and dust. Impurities on the surface were verified by Auger electron spectroscopy (Fig. 1) to be below the 1% detection limit. However, the compositional ratio of the initial state of an oxide material may be influenced by sputtering condition, and results in the various types of surface at the beginning of the experiment. This can be verified by measuring the relative Auger signal ratio of Zn to O at different Ar ion energies. After the ratios were normalized by the bulk sensitivities, a linear dependence of the concentration ratio with the ion energy was revealed. Fig. 2 depicts this relation. The surface concentration of Zn is always greater than that of O. Although Zn has a larger sputtering yield than O [10], the deficiency of O phase is favorable. The oxygen vacancy results in the formation of an N-type ZnO(002) semiconductor [18]. Therefore, high-energy Ar⁺ sputtering generated an O-deficient surface. The resulting Zn-type ZnO(002) surface was served as the substrate for subsequent experiments in this study.

2.2. Calibration of the Co ultra-thin film deposition rate

Fig. 3 depicts the growth of Co monitored by AES on the ZnO(002) substrate. In Fig. 3(a), the Co signal shows an exponential increase, indicating that the growth of Co follows the Volmer-Weber (VW) 3D island growth mode. The Co thickness was estimated by the Auger electron intensities of the elements, bulk intensities from the AES handbook, inelastic electron mean free paths (IMFPs) for the constituent, and backscattering factors [19–21]. Although the thickness of Co films was a minor parameter, the deposition rate of Co was calibrated by the ratio of Auger intensities of Co to ZnO versus time

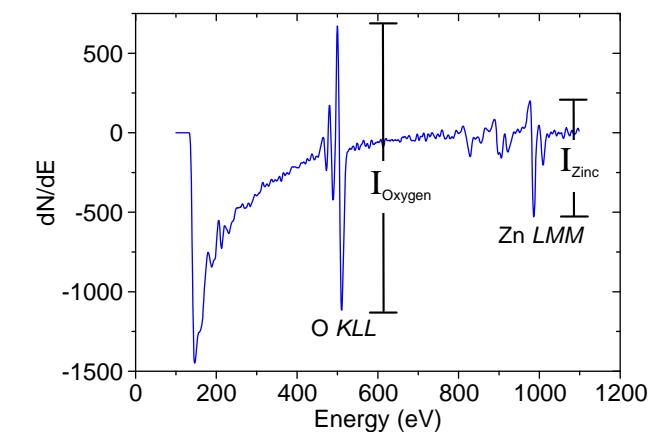


Fig. 1. The Auger spectrum of the clean ZnO(002) substrate after 1 keV Ar⁺ sputtering for 1 h.

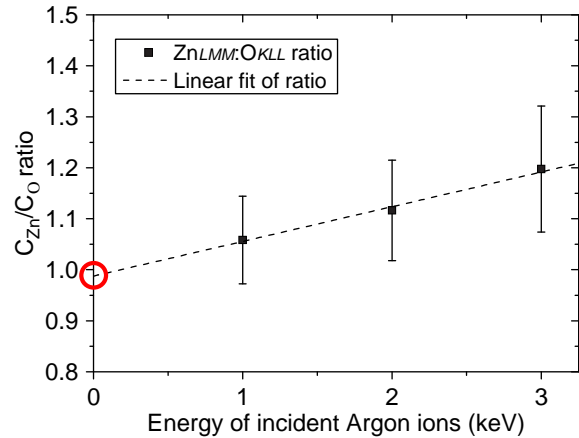


Fig. 2. The composition ratio of Zn to O recorded by different Ar⁺ energies.

given in Fig. 3(b). The largest IMFP within the three elements in the Co/ZnO sample occurred in the electron path of Zn LMM transition around the peak of 985 eV. A clear break appeared at approximately 34 h. This break point corresponds to the point at which the deposited Co thickness exceeds that of the inelastic mean free path of Zn, which the NIST database shows to be approximately 1.97 nm [20]. The

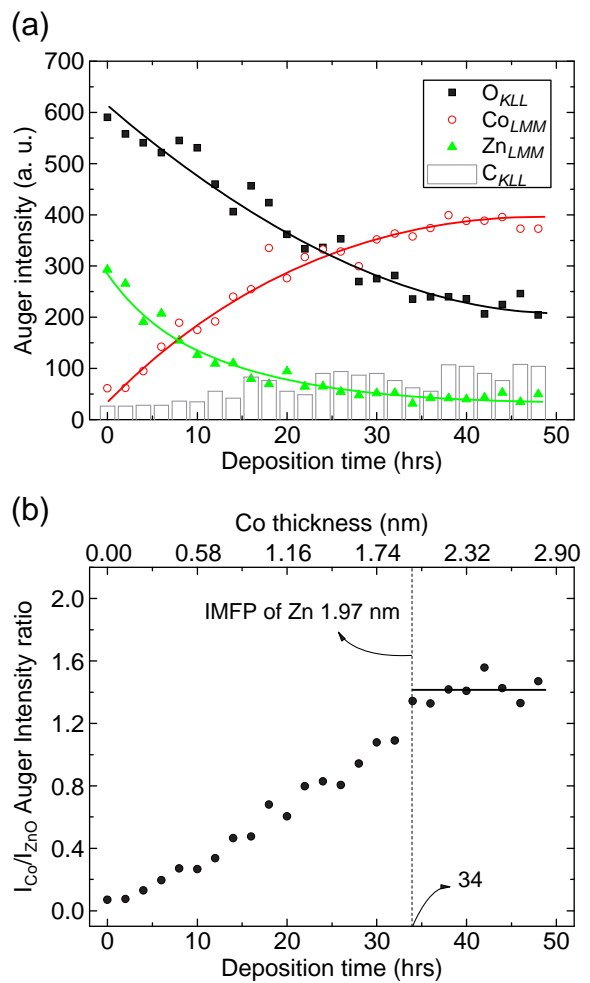


Fig. 3. (a) The relative Auger intensities of Co, Zn, and O varied with time during the deposition of Co, and (b) calculated ratio of Co to the bulk signal Zn and O Auger intensities versus the deposition time. Auger intensities in (b) were normalized by elemental sensitivities. The curve breaks at around 34 h. This time point was used to estimate and calibrate the thickness of Co films.

variation of the ratio of Co to ZnO began to fluctuate after 34 h. This study assumes that the Co thickness equaled 1.97 nm at that time point to calibrate the thickness of other Co films based on a constant growing rate. Previous research indicates that thickness estimation is reliable to within 5% in ultra-thin films [22]. The experiments in this study limit the thickness of Co to less than 2 nm, and confirm that the largest ratio is approximately 2.54. For instance, the thickness of the largest ratio was estimated at 1.7 nm and the deposition rate was estimated at about 0.58 Å/h. Since the growth of Co films followed the VW mode, a low deposition rate helps prevent the Co clusters aggregating on the surface.

3. Results and discussion

The experiments in this study fabricated CoN_x ultra-thin films on the Co/ZnO(002) template by the bombardment of nitrogen plasma. The following subsections describe the experimental process and physical properties of Co–N films through tuning the ion parameters.

3.1. Formation of Co–N films on ZnO(002) by N^+ ion sputtering

This subsection compares the targets of the clean ZnO(002) and the Co covered ZnO to determine the effects of N ion sputtering in fabricating N-based films. Fig. 4 compares four spectra in which the Auger peaks of Co, Zn, O, and N constituents appear in the AES spectra with or without N^+ sputtering at an ion energy of 500 eV. Fig. 4(a) shows N plasma bombarded on the clean ZnO(002) for short (spectrum (1)) and long (spectrum (2)) periods. Spectrum (3) in Fig. 4(b) is the sample covered with Co film only. Notice that the N signal only appears in spectrum (4), which corresponds to the ZnO(002) covered by Co. It is easy to compare the N KLL Auger peak intensity at around 383 eV before and after Co covering, as Fig. 4(a) and b illustrates, respectively. Consequently, the emergence of N only affects the upper adsorbate layers. How the Co–N films form on the ZnO surface remains unclear. This study also examines whether the ZnO substrate contributes to the effect of nitridation. The following

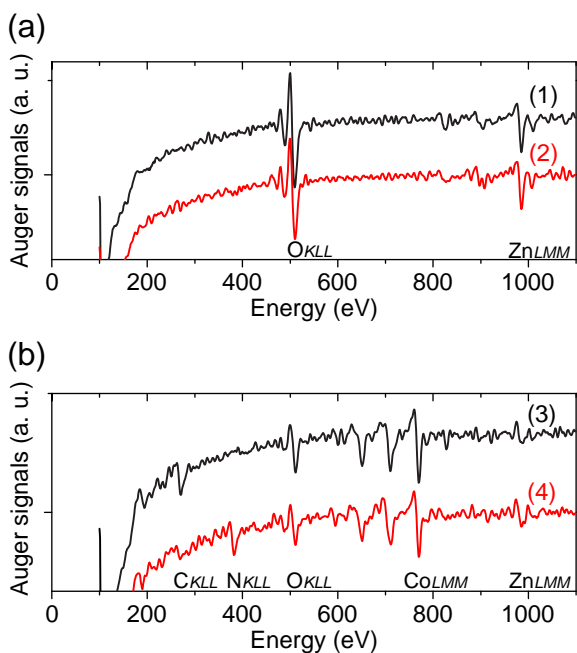


Fig. 4. Comparison of the Auger spectrum, indicating whether the surfaces were covered by Co films with a fixed ion energy of 500 eV: (a) clean ZnO(002) , and (b) 1.4 nm Co/ZnO(002) . The spectra corresponding to the (1) clean ZnO sputtered by 500 eV N^+ 7.5 min, (2) clean ZnO sputtered by 500 eV N^+ 60 min, (3) Co/ZnO(002) , and (4) Co/ZnO(002) sputtered by 500 eV N^+ 7.5 min.

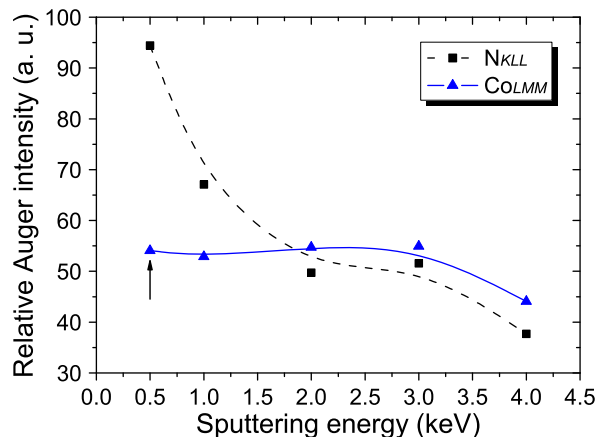


Fig. 5. The variation of relative Auger intensities of Co and N versus the ion energy of N^+ . The intensity ratio for an ion energy was measured after 7.5-min sputtering.

subsection shows that Co ultra-thin films not only act like a sponge to absorb nitrogen, but also play an important role in affixing nitrogen to the ZnO(002) surface.

3.2. Ion energy and sputtering time dependence in N^+ ion sputtering

To observe the effect of ion energies, the acceleration voltage of N^+ was varied from 0.5 to 4 keV. The ion current on the control panel was maintained at approximately 20 μA via controlling the vacuum pressure accurately using an UHV leak valve. Fig. 5 illustrates the relative N and Co Auger peak intensities after the preliminary 7.5-min sputtering as a function of N^+ energy tested on the 0.2 nm Co/ZnO(002) sample by AES in our case. The largest intensity ratio of N to Co was approximately 1.75 at 500 eV. The ratio of N to Co decreased as the ion energy increased. The implantation effect of ions into a solid is typically favorable in high-energy bombardment [23], while the implantation of N is promoted in low energy. This opposite effect of N^+ energy may be caused by the competition between implantation and sputtering phenomena for the surface. The phenomenon motivated us to observe more about how to enrich the nitrogen amount in the ultra-thin Co films. Since the largest composition of N occurred at 500 eV, the sputtering process should exhibit a time-dependent effect. The Auger peak intensities of the 1.4 nm Co/ZnO films were recorded after 7.5-min sputtering period to determine the composition variation in the process, as shown in Fig. 6. The period was adjusted because the intensity ratio of Co and N saturated approximately after 150 min.

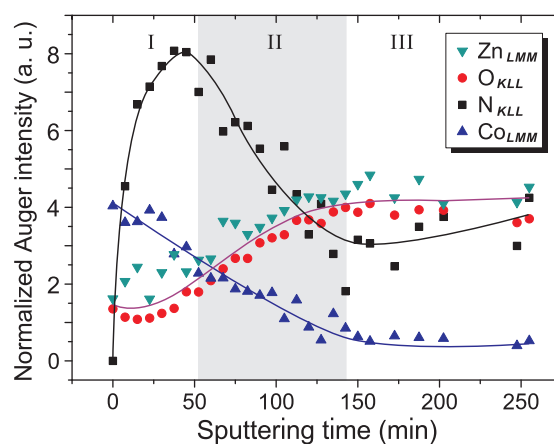


Fig. 6. The normalized Co, N, Zn, and O Auger intensities of 1.4 nm Co/ZnO(002) varied with the sputtering time during 500 eV N^+ sputtering.

The measured Auger peak intensities were calibrated from the corresponding bulk intensities to determine the variations of surface compositions [19]. The curves in Fig. 6 include three distinct regions. In region I, the rapid increase of the N signal indicates that the implantation effect of N ions is related to the formation of Co–N layers. A decrease in the Co signal accompanies the sputtering effect to the Co layers. In region II, the nitrogen signal reaches its maximum value at about 40 min. The Co signal decreases monotonically. After 40 min, the Co and N signals both decrease gradually. In region III, most Co atoms have been sputtered on the surface. The Co signals reduced to the background, leaving only a little N on the ZnO surface. Compared to the bare ZnO(002) without a Co covering, the long N⁺ sputtering time does not generate a N trajectory on the ZnO surface, as Fig. 4(a) indicates. This shows that Co covering films play an important role in affixing N to the ZnO surface.

Region II clearly shows that the reducing rate in Auger intensity of Co or N signal follows an exponential decay. After applying natural logarithm to the y-axis scale, the intensities versus the sputtering time reveal an inversely linear relationship. The left side of Fig. 7 illustrates this analysis. The slope values of Co and N are close. This means that the logarithm signals of Co and N decrease with the same sputtering rate. The thickness of the upper Co–N layers in region II depletes without any obvious changes in the surface composition of Co_qN_x. The samples were analyzed using low-energy electron diffraction and I–V measurement, which found no diffraction pattern or spots. In this case, the surface structure has lost its long-range order. This proves that an amorphous phase is highly possible in the sputtering process. Hence, the composition of amorphous Co_qN_x was estimated based on the Vegard's law which assumes homogeneous composition in multicomponent materials, as the right side of Fig. 7 indicates [24].

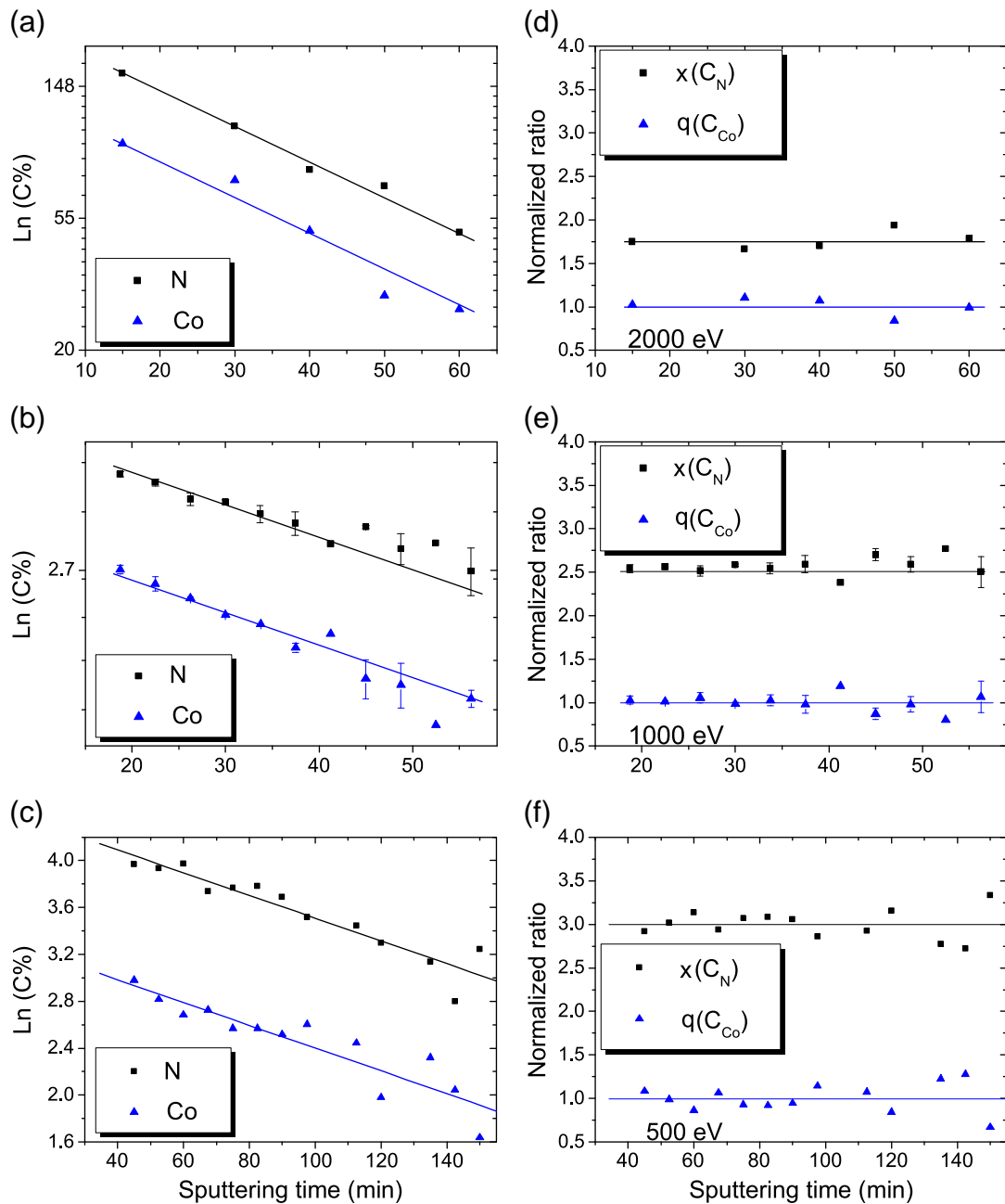


Fig. 7. The variation of the Co and N Auger intensities in the defined region II versus the sputtering time recorded at different ion energies E , where E represents (a) 2000 eV, (b) 1000 eV, and (c) 500 eV. The y-axis in the figure was changed to a natural logarithm scale. The composition ratios x of Co_qN_x were then manipulated according to Eq. (5) and indicated at the right side (d)–(f), where q was normalized to 1.

All the Co signals were normalized to 1. The formation of CoN_x films was non-stoichiometric. According to previous research of Co-N compounds, the rich structural phases of the compounds like CoN , Co_2N , Co_3N , Co_4N , may be stoichiometric under high-pressure radio-frequency sputtering techniques [25]. In that case, the N amount is probably less than the Co amount. However, relatively few papers discuss about Co_qN_x compounds with abundant nitrogen (i.e., $x > q$).

Ion energy may be the key factor to obtain a rich N composition. Therefore, the time-dependent experiment with the same thickness of Co film was repeated with different ion energies varying at 1 and 2 keV. These experiments revealed similar behaviors in various ion energies. After applying a natural logarithm for the scale of the Auger intensity, indicated as the region in gray color in Fig. 6, these data were recorded and compared in the left column of Fig. 7. The variations in Fig. 7(a) to (c) correspond to the experiment done by the ion energies of 2000, 1000, and 500 eV. The linear relationship in these figures indicates that the constant composition ratio of N to Co depends on the ion energy in the sputtering process. If the thickness of the amorphous CoN_x film in an ion energy depletes exponentially via the following equations, the sputtering formula for each constituent can be expressed as

$$R_N / R_N^0 = e^{-k_N t} \quad (1)$$

$$R_{\text{Co}} / R_{\text{Co}}^0 = e^{-k_{\text{Co}} t} \quad (2)$$

Application of natural logarithms on both sides results in

$$\ln R_N - \ln R_N^0 = -k_N t \quad (3)$$

$$\ln R_{\text{Co}} - \ln R_{\text{Co}}^0 = -k_{\text{Co}} t \quad (4)$$

if the slopes $k_N = k_{\text{Co}}$, then

$$\frac{R_N^0}{R_{\text{Co}}^0} = \frac{R_N}{R_{\text{Co}}} = x, \quad (5)$$

where R is the normalized Auger peak intensity and t is the sputtering time. This means that choosing a certain ion energy can maintain a certain composition x in the sputtering process. The parameter k contains information about the sputtering cross section, ion flux density, and even sputtering yield [26]. The constant slope values in Fig. 7(a)–(c) represent that Co and N have the same sputtering cross section. The behavior is consistent to our previous studies [17]. The sputtering yield is proportional to the sputtering cross section. The ratio of sputtering yield to sputtering cross section equals the coverage or initial composition of the constituent. Since the ion flux density remains constant within the sputtering, the linear slopes of Co and N in region II correspond to the time-independent composition x of CoN_x films.

Different ion energies can generate various CoN_x compositions. The chemical formula of Co-N film represents as Co_qN_x , where subscript q is normalized to 1. From Eq. (1) to (5), the time-dependent ratios in Fig. 7(a)–(c) can be transformed to the compositions in Fig. 7(d)–(f) to compare the effect of ion energies. The ratios of N to Co with rich N amount from 1.7, 2.5, and 3.0 were obtained at ion energies of 2000, 1000, to 500 eV, respectively. This means that the ion energy can tune the composition of CoN_x in which the thickness is less than 2 nm.

Notice that ion implantation in semiconductors typically utilizes greater ion energy to force the ion impurities into thin films or substrate surfaces [27,28]. However, the N ratios in this study show the opposite phenomenon; the largest composition of N occurs at the lowest ion energy. Fig. 8(a) depicts the relationship of composition ratio R to ion energy E . The composition ratio R is dominated by the empirical law which indicates as $R_N/R_{\text{Co}} = x = -k' \cdot E$, where k' contains the structural factors within the sputtering in this system. The ion energy controls the compositional ratio. When the ion energy decreased from 2000 to 500 eV, the ratio x reversely increased from

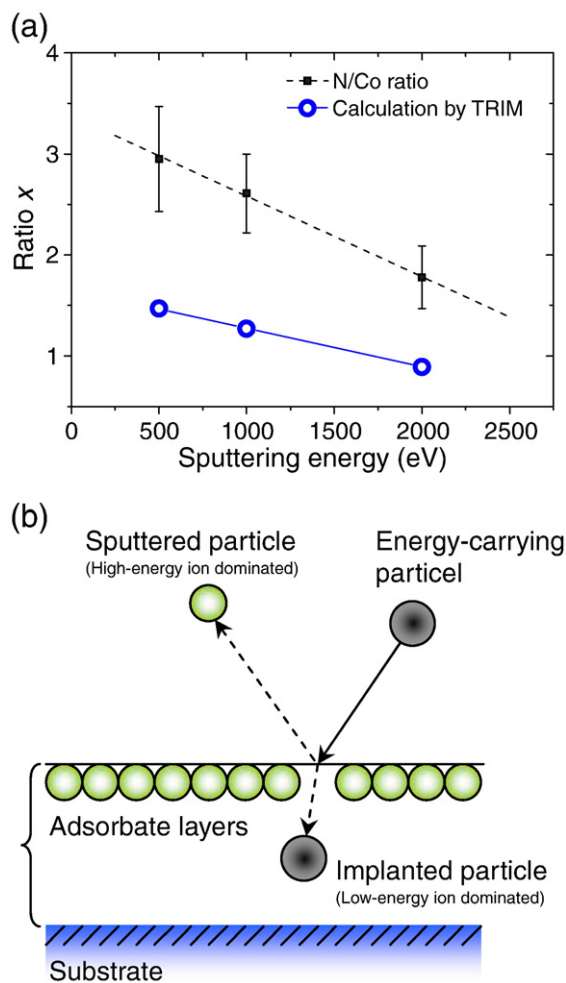


Fig. 8. (a) The composition ratio x of Co_qN_x versus the ion energy based on the results of Fig. 7(d) to (f). The open circles are the simulation results by TRIM code based on the ratios of the sputtering yield as the experimental composition in Fig. 7. (b) Schematic diagram of the Co-N films formed in the N^+ sputtering process. The implantation and sputtering effects occurred simultaneously, and were dominated by low-energy and high-energy ions, respectively.

1.7 to 3.0. This is likely due to the competition between the implantation and sputtering effects on the surface layers. In the low-energy ion sputtering, our results showed that the implantation effect was obviously larger than the sputtering effect. Hence, the technique promotes to fabricate an N-rich solid thin film in a low-energy region. Fig. 8(b) shows a schematic diagram that the inductive inference is focused on the effect of ion energy.

The conclusion about the sputtering effect greater than the implantation effect (mixing effect) at a high ion energy is in good agreement with the calculation by Transport of Ions in Matter (TRIM) code. Our simulation data are listed in Table 1 and compare with the

Table 1

Results of CoN_x compositions with N^+ ion energy by the presented experiment and TRIM calculation (simulation type: surface sputtering/monolayer collision steps). The three-layer structure in the simulation is Co_qN_x -amorphous layer of 2 Å (4.2149 g/cm³), ZnO-amorphous layer of 20 Å (4.283 g/cm³), and ZnO-crystal layer of 10000 Å (5.606 g/cm³) from the top of the surface. The total bombarding ions are 5000. The densities except for the ZnO-crystal layers are suggested in the program and not very accurate.

Ion energy (keV)	Composition (Expt.)	Composition (Calc.)
0.5	CoN_3	$\text{Co}_{40.5}\text{N}_{59.5}$ ($\text{CoN}_{1.47}$)
1	$\text{CoN}_{2.5}$	$\text{Co}_{44}\text{N}_{56}$ ($\text{CoN}_{1.27}$)
2	$\text{CoN}_{1.75}$	$\text{Co}_{53}\text{N}_{47}$ ($\text{CoN}_{0.89}$)

experimental result in Fig. 8(a). The ratios of the sputtering yield Y , i.e. Y_N/Y_{Co} , in simulation are kept and follow the result of average compositions in Fig. 7. Sputtering cross section of Co or N was assumed to a constant. For instance, sputtering effect in ion energy of 2 keV for the thin surface layer ($CoN_{0.89}$) is more effective than that of 500 eV for the layer ($CoN_{1.47}$) because we observed that the amount of N residue on the surface at 2 keV is less than that at 500 eV.

For the surface sputtering, sputtering yield is an indispensable parameter in the discussion. To obtain a calculated sputtering yield as a function of ion energy, stoichiometric composition has to be defined. However, the surface layers may be amorphous by cyclic sputtering. The average roughness of the ZnO(002) crystal surface was estimated around 2 nm from the test report. For a multicomponent target, one atom may sputter preferentially over the other. Hence the surface will be depleted in this atom. The phenomenon "preferential sputtering" will be occurred. Unfortunately, this reaction is not included in the TRIM calculation and the calculation agrees in most cases at high-energy cascades. Since the experiment was performed at around room temperature, further studies considering the chemical driving forces of ions and ion-induced solubility with the magnitude of the heat of ion mixing in the bombardment are needed [29]. Although the experimental compositions of CoN_x are nearly two times the simulation values, the behaviors of the sputtering yield in terms of ion beam energy in the presented experimental data and simulation are consistent with the studies of low-energy ion bombardment (<5 keV) [30]. The only difference represents here that the N ions are directly reacting with the surface layers, i.e. the Co films, in which the reaction forms CoN_x first and the nitride film is depleted further. During the sputtering process, the chemical bonding even in the amorphous CoN_x phase may have formed. The bonding force strength may affect the final composition x . This may explain the reason why the result of composition in experiment and simulation was deviated. Due to the competition between implantation and sputtering effects in the ion bombardment, prolonged low-energy N^+ bombardment produces Co–N compounds with an enriched phase of N. In other words, adjusting the ion energy of nitrogen to generate nitride-based films is effective and obtaining an exactly surface composition in expected thickness is feasible in the ultra-thin film technology.

4. Conclusion

This study demonstrates a sputtering technique for generating different ion energies of nitrogen between 0.5 and 2 keV and utilizes reactive ionized gas to form nitride-based ultra-thin Co–N films on the ZnO(002) surface. The time-dependent sputtering experiments in this study show that nitrogen signals accumulated on the ZnO surface upon Co films covering. The nitrogen amount is saturated immediately when the CoN_x phase forms in the initial sputtering. When the ratio of Co to N is saturated, the thickness of the surface layers of CoN_x depletes with the sputtering time without changing its composition. The constant ratio of x is strongly related to the incident ion energy. The ratio of N and Co compositions increases as the ion energy of

nitrogen decreases. This makes the fabrication of N-based ultra-thin films possible by adjusting the ion-generated energy. At the same time, the distinct thickness of ultra-thin nitride layers can be achieved without changing its composition during direct-current ion sputtering in ultrahigh vacuum.

Acknowledgements

Authors acknowledged the grant support from the National Science Council Taiwan Republic of China under project numbers NSC98-2112-M-415-003-MY3 and 96-2112-M-415-005-MY2. Authors would also thank Professor Y.-H. Lee from National Cheng Kung University for a fruitful discussion and gave a positive suggestion for this study.

References

- [1] J.K. Hirvonen, *Annu. Rev. Mater. Sci.* 19 (1989) 401.
- [2] M. Akbulut, N.J. Sack, T.E. Madey, *Surf. Sci. Rep.* 28 (1997) 177.
- [3] H. Niehus, W. Heiland, E. Taglauer, *Surf. Sci. Rep.* 17 (1993) 213.
- [4] S.T. Picraux, *Annu. Rev. Mater. Sci.* 14 (1984) 335.
- [5] J.R. Conrad, J.L. Radtke, R.A. Dodd, F.J. Worzala, N.C. Tran, *J. Appl. Phys.* 62 (1987) 4591.
- [6] T. Kim, K. Alberi, O.D. Dubon, M.J. Aziz, V. Narayanamurti, *J. Appl. Phys.* 104 (2008) 113722.
- [7] R. Capelletti, A. Miotello, P.M. Ossi, *J. Appl. Phys.* 81 (1997) 146.
- [8] J. Jagielski, M. Kopcewicz, G. Gawlik, W. Matz, L. Thomé, *J. Appl. Phys.* 91 (2002) 6465.
- [9] K. Nakajima, S. Okamoto, T. Okada, *J. Appl. Phys.* 65 (1989) 4357.
- [10] J.F. Ziegler, J.P. Biersack, U. Littmark, *SRIM – The Stopping and Range of Ions in Matter-SRIM*, Pergamon Press, New York, 2009.
- [11] K. Kurihara, S.-I. Hikino, S. Adachi, *J. Appl. Phys.* 96 (2004) 3247.
- [12] R.G. Gordon, H. Bhandari, H. Kim, "Cobalt nitride layers for copper interconnects and methods for forming them", US patent No. WO/2009/088522.
- [13] Y. Takeda, M. Nishijima, M. Yamahata, K. Takeda, N. Imanishi, O. Yamamoto, *Solid State Ionics* 130 (2000) 61.
- [14] H.K. Cheng, Y.Q. Huang, A.Q. Wang, X.D. Wang, T. Zhang, *Top. Catal.* 52 (2009) 1535.
- [15] M. Matsuoka, K. Ono, T. Inukai, *Appl. Phys. Lett.* 49 (1986) 977.
- [16] C.W. Su, M.S. Huang, Y.C. Chang, T.H. Tsai, Y.H. Lee, J.C. Lee, *Chin. J. Phys.* 47 (2009) 370.
- [17] C.W. Su, M.S. Huang, Y.C. Chang, T.H. Tsai, Y.H. Lee, J.C. Lee, *J. Appl. Phys.* 105 (2009) 033509.
- [18] T. Tatsumi, M. Fujita, N. Kawamoto, M. Sasajima, Y. Horikoshi, *Jpn. J. Appl. Phys.* 43 (2004) 2602.
- [19] L.E. Davis, N.C. MacDonald, P.W. Palmberg, G.E. Riach, R.E. Weber, *Handbook of Auger electron spectroscopy*, 2nd ed. Physical Electronics Division, Minnesota, 1978.
- [20] C.J. Powell, A. Jablonski, NIST electron inelastic-mean-free-path database version 1.1, National Institute of Standards and Technology, Gaithersburg, MD, 2000.
- [21] D. Briggs, M.P. Seah, *Practical Surface Analysis*, 2nd Ed., John Wiley & Sons, New York, 1990, p. 205, Ch. 5.
- [22] C.W. Su, H.Y. Ho, C.S. Shern, R.H. Chen, *Thin Solid Films* 425 (2003) 139.
- [23] S.O. Kucheyev, J.S. Williams, S.J. Pearton, *Mater. Sci. Eng.* 33 (2001) 51.
- [24] A.R. Denton, N.W. Ashcroft, *Phys. Rev. A* 43 (1991) 3161.
- [25] K. Oda, T. Yoshio, K. Oda, *J. Mater. Sci.* 22 (1987) 2729.
- [26] H.F. Winters, E. Taglauer, *Phys. Rev. B* 35 (1987) 2174.
- [27] M. Mikulics, E.A. Michael, M. Marso, M. Lepsa, A. van der Hart, H. Lüth, A. Dewald, S. Stanček, M. Mozolik, P. Kordoš, *Appl. Phys. Lett.* 89 (2006) 071103.
- [28] H. Pelletier, D. Müller, P. Mille, A. Cornet, J.J. Grob, *Surf. Coat. Technol.* 151–152 (2002) 377.
- [29] R. Kelly, A. Miotello, *Appl. Phys. Lett.* 64 (1994) 2649.
- [30] V.S. Smentkowski, *Prog. Surf. Sci.* 64 (2000) 1.